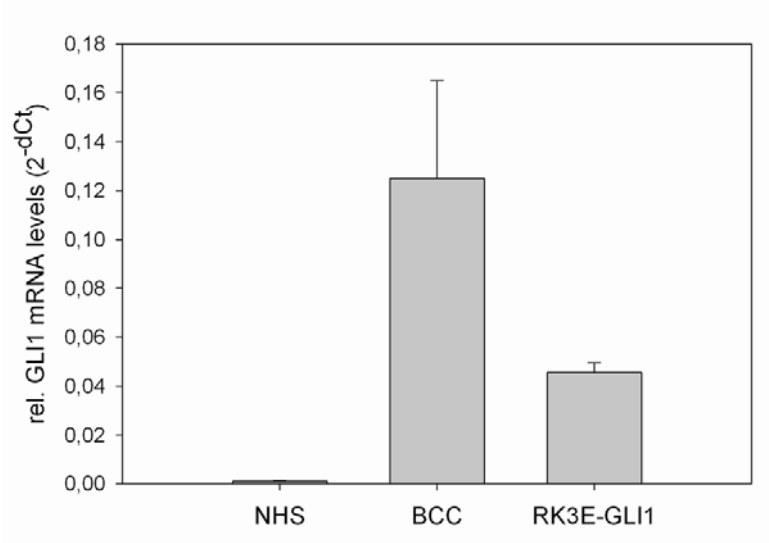
0,18
0,16
0,14
0,12
0,10
0,08
0,06
0,04
0,02
0,00
rel. GLI1 mRNA levels (2-dCt)
NHS
BCC
RK3E-GLI1

Figure S1

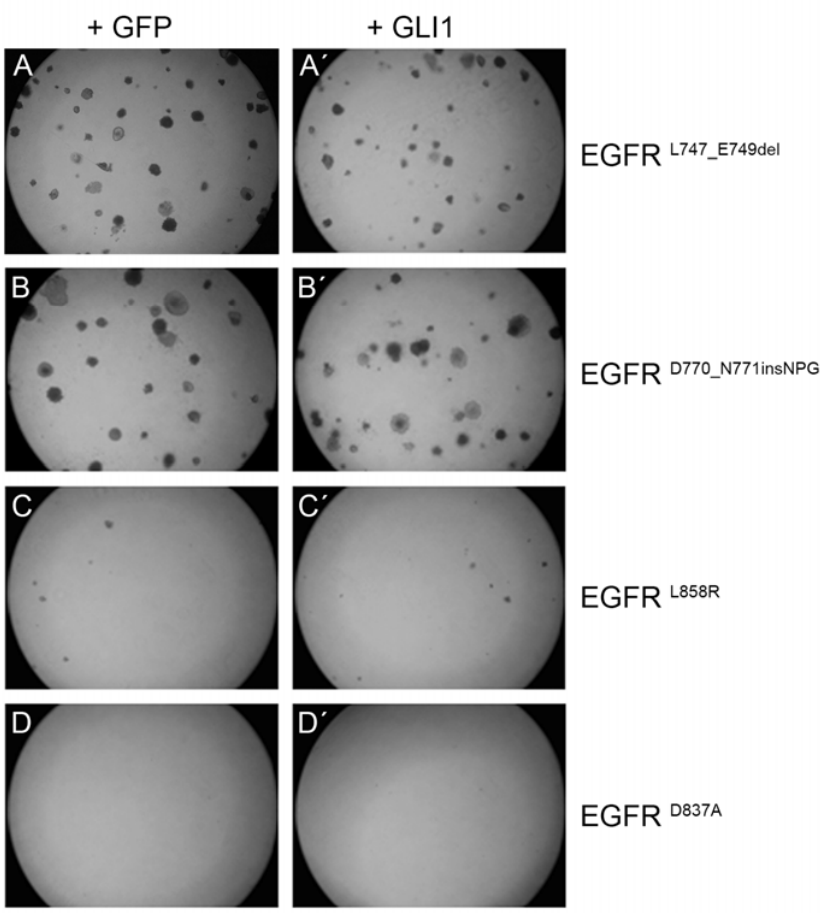
+ GFP
+ GLI1
A
A´
EGFR L747_E749del
B
B´
EGFR D770_N771insNPG
C
C´
EGFR L858R
D
D´
EGFR D837A

Figure S2

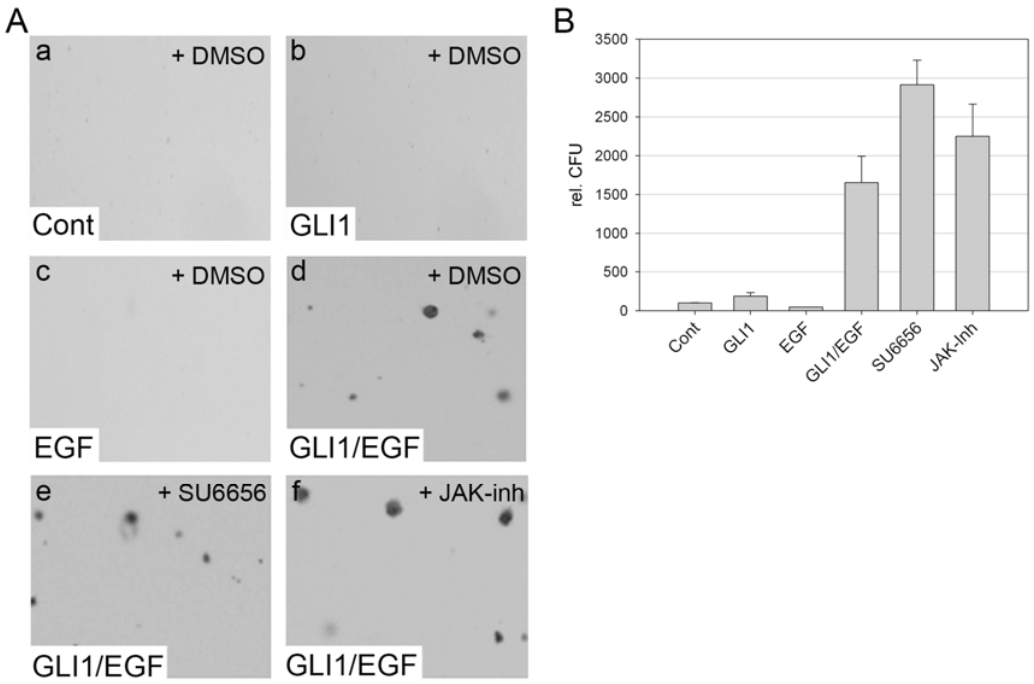
A
a
+ DMSO
Cont
b
+ DMSO
GLI1
c
+ DMSO
EGF
d
+ DMSO
GLI1/EGF
e
+ SU6656
GLI1/EGF
f
+ JAK-inh
GLI1/EGF
B
rel. CFU
3500
3000
2500
2000
1500
1000
500
0
Cont
GLI1
EGF
GLI1/EGF
SU6656
JAK-Inh

Figure S3

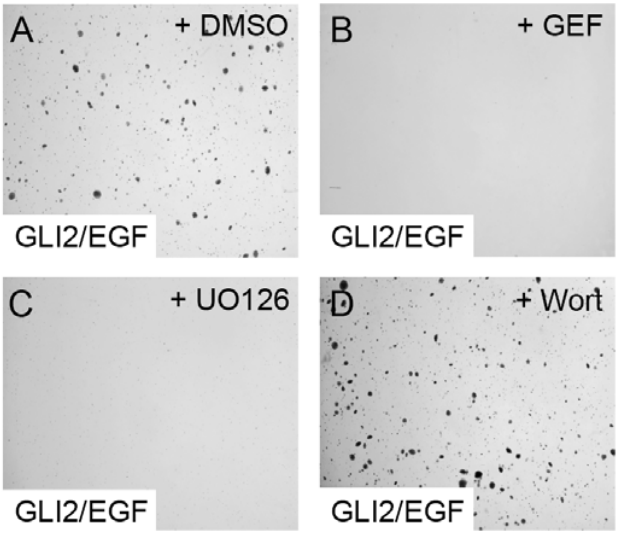

Figure S4

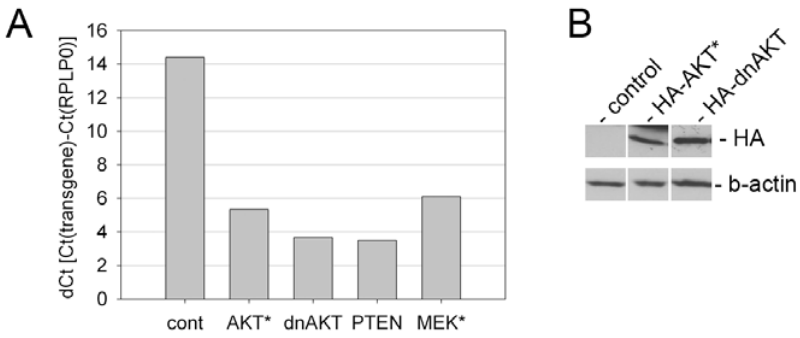
A
dCt [Ct(transgene)-Ct(RPLP0)]
16
14
12
10
8
6
4
2
0
cont
AKT*
dnAKT
PTEN
MEK*
B
- control
- HA-AKT*
- HA-dnAKT
- HA
- b-actin

Figure S5

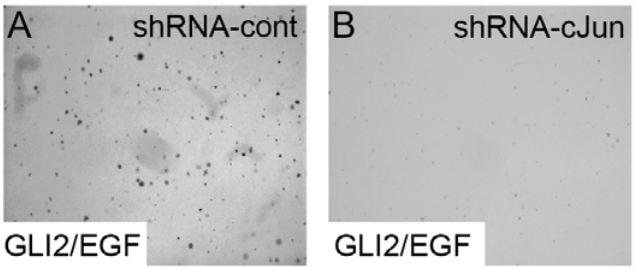

Figure S6

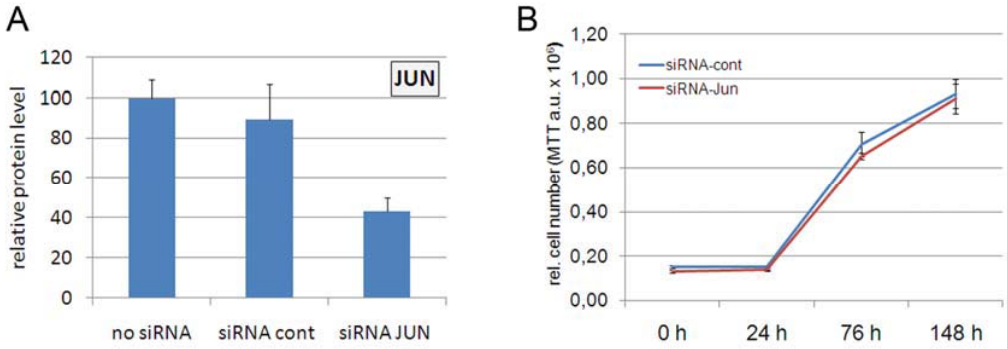
A
JUN
relative protein level
120
100
80
60
40
20
0
no siRNA
siRNA cont
siRNA JUN
B
siRNA-cont
siRNA-Jun
rel. cell number (MTT a.u. x 10³)
1,20
1,00
0,80
0,60
0,40
0,20
0,00
0 h
24 h
76 h
148 h

Figure S7

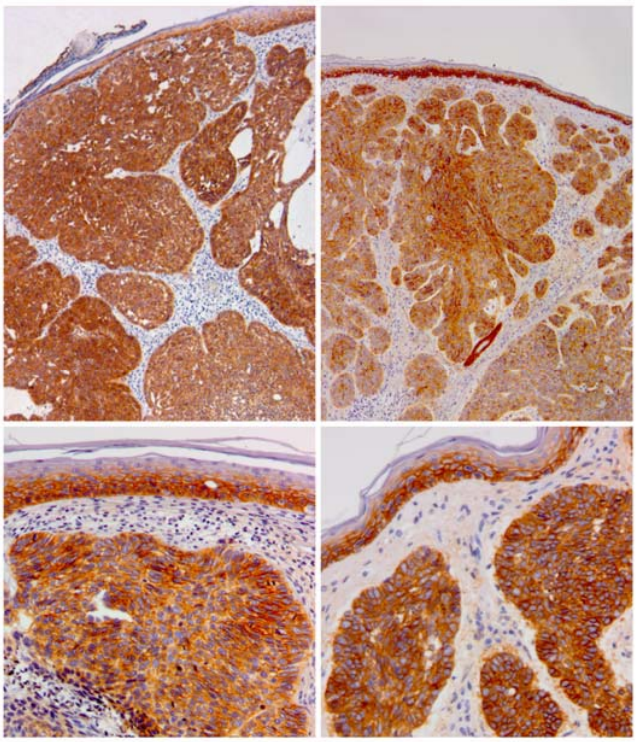

Figure S8

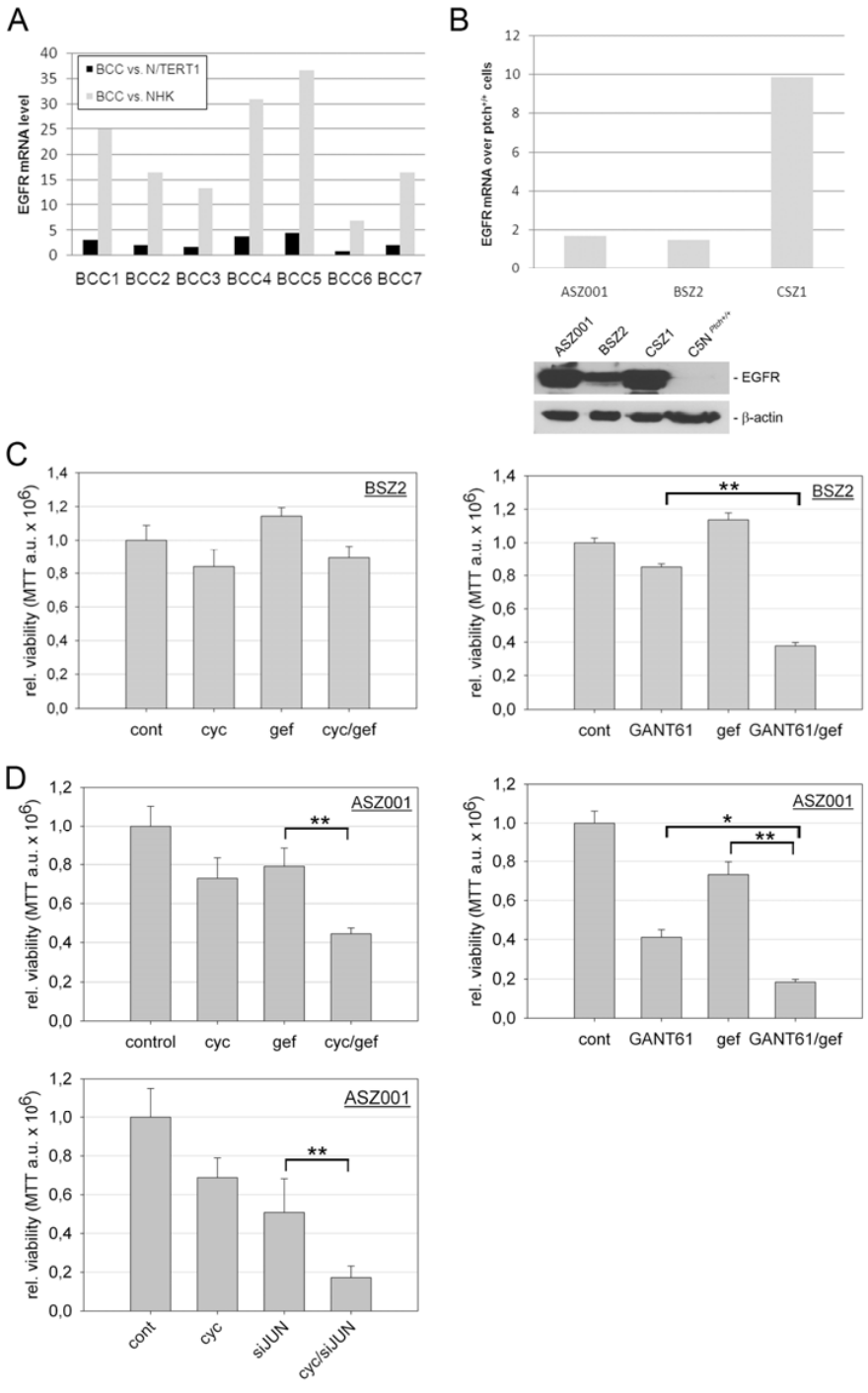
A
EGFR mRNA level
BCC vs. N/TERT1
BCC vs. NHK
BCC1 BCC2 BCC3 BCC4 BCC5 BCC6 BCC7
B
EGFR mRNA over ptch+/+ cells
ASZ001
BSZ2
CSZ1
ASZ001
BSZ2
CSZ1
C5N Ptch+/+
- EGFR
- β-actin
C
rel. viability (MTT a.u. x 10^6)
BSZ2
cont
cyc
gef
cyc/gef
**
BSZ2
cont
GANT61
gef
GANT61/gef
D
ASZ001
**
control
cyc
gef
cyc/gef
ASZ001
*
**
cont
GANT61
gef
GANT61/gef
ASZ001
**
cont
cyc
siJUN
cyc/siJUN

Figure S9

Table I: GLI and AP-1 binding sites in promoters of EGF-independent and dependent GLI target genes

GENE	GLI binding site (Reference)	AP-1 binding site	position rel. to TSS	Reference
BCL2	Regl et al. (2004)	neg.	--	
PTCH	Agren et al. (2004)	neg.	--	
IL1R2	Kasper et al. (2006)	tgactca	-1362	predicted
S100A9	Kasper et al. (2006)	tgactca	-2577	predicted
JAG2	Kasper et al. (2006)	tgactca	-4466	predicted
CCND1	Kasper et al. (2006)	tgactca/tgaggtaa	-954/-52	Albanese et al., 1995; Herber et al., 1994;

References:

Agren M, Kogerman P, Kleman MI, Wessling M, Toftgard R (2004) Expression of the PTCH1 tumor suppressor gene is regulated by alternative promoters and a single functional Gli-binding site. *Gene* **330:** 101-114

Albanese C, Johnson J, Watanabe G, Eklund N, Vu D, Arnold A, Pestell RG (1995) Transforming p21ras mutants and c-Ets-2 activate the cyclin D1 promoter through distinguishable regions. *J Biol Chem* **270**(40)**:** 23589-23597

Herber B, Truss M, Beato M, Muller R (1994) Inducible regulatory elements in the human cyclin D1 promoter. *Oncogene* **9**(4)**:** 1295-1304

Kasper M, Schnidar H, Neill GW, Hanneder M, Klingler S, Blaas L, Schmid C, Hauser-Kronberger C, Regl G, Philpott MP, Aberger F (2006) Selective modulation of Hedgehog/GLI target gene expression by epidermal growth factor signaling in human keratinocytes. Mol Cell Biol 26(16): 6283-6298.

Table S2: EGFR protein expression in BCC

BCC ID	EGFR	BCC subtype
1	++	nodular
2	+	nodular
3	+++	infiltrating
4	++	infiltrating
5	+++	nodular
6	+	nodular
7	++	nodular
8	+++	nodular
9	+	nodular
10	+++	nodular
11	++	nodular
12	+++	nodular
13	++	nodular
14	+	nodular
15	+++	nodular
16	++	nodular
17	++	nodular
18	+	nodular
19	+++	nodular
20	++	nodular

-	absent
+	weak (lower signal than in normal epidermis)
++	moderate (signal comparable to level in normal epidermis)
+++	high (stronger signal than in normal epidermis)

Supplementary figure S1: Relative mRNA expression levels of human GLI1 in normal human skin (NHS), BCC and transduced RKE3 cells (RK3E-GLI1).

Supplementary figure S2: STAT3/5 and AKT dependent oncogenic EGFR variants $EGFR^{L747\_E749del}$ and $EGFR^{D770\_N771insNPG}$ and to a lesser extent $EGFR^{L858R}$ induce transformation but do not synergize with GLI1 in RK3E cells. The kinase-dead mutant $EGFR^{D837A}$ was used as negative control. Following transduction with the indicated EGFR variants, cells were subsequently transduced with GFP (+GFP, A-D)) or GLI1 (+GLI1, A´-D´) expressing retrovirus.

Supplementary figure S3: (A) Pharmacological blockade of SRC (e) and JAK (f) function by SU6656 and JAK inhibitor I (JAK-inh) treatment, respectively, does not affect transformation in response to combined EGFR and GLI activation. (B) Quantitative analysis of soft agar cultures shown in (a-f).

Supplementary figure S4: Anchorage-independent growth of doxycycline-inducible GLI2 HaCaT keratinocytes by integration of EGFR and GLI2 activity. (A) Anchorage-independent growth in response to combined EGFR/GLI2 activation. Inhibition of EGFR function by gefitinib (GEF) (B) or MEK1/2 function by UO126 treatment (C) dramatically reduces colony growth in soft agar induced by concurrent EGFR and GLI2 activation, while inhibition of PI3K/AKT function by wortmannin treatment (+ Wort) had no effect (D). A dominant active form of GLI2 lacking part of the N-terminus was expressed by addition of doxycycline to the culture.

Supplementary figure S5: (A) qPCR analysis of cells transduced with dominant active AKT*, dominant negative AKT (dnAKT), PTEN or dominant active MEK (MEK*) expression constructs; note that the smaller the value the higher the expression is. Expression of RPLP0 was used as reference control. (B) Western blot showing efficient expression of HA-tagged AKT* and dnAKT* constructs used in Figure 4A-D.

Supplementary figure S6: siRNA knock-down of JUN abolishes anchorage-independent growth induced by concurrent activation of EGFR and GLI2 expression. Soft agar assays of doxycycline-inducible GLI2 expressing HaCaT keratinocytes treated with EGF (GLI2/EGF) and expressing non-specific control shRNA (shRNA-cont) (A) or JUN-specific shRNA (shRNA-cJun) (B). A dominant active form of GLI2 lacking part of the N-terminus was used. Stable knock-down was achieved by retroviral expression of JUN shRNA.

Supplementary figure S7: stable siRNA knock-down of JUN does not affect HaCaT keratinocyte proliferation in vitro. (A) Quantitative analysis of JUN protein expression in response to control (siRNA cont) or JUN specific siRNA (siRNA JUN). Stable knock-down was achieved by retroviral expression of respective shRNA constructs. (B) Growth curve of HaCaT keratinocytes stably expressing control (siRNA-cont) or JUN siRNA (siRNA-Jun).

Supplementary figure S8: Representative BCC stainings showing specific expression of EGFR in the tumor islands and adjacent non-lesional epidermis.

Supplementary figure S9: (A) qPCR analysis of EGFR mRNA expression in seven BCC samples (BCC1-BCC7) compared to EGFR mRNA expression in N/TERT1 or normal human keratinocytes (NHK). (B) qPCR analysis of EGFR mRNA (upper panel) and EGFR protein expression (lower panel) in mouse BCC cell lines ASZ001, BSZ2, CSZ1 compared to EGFR expression in patched $^{+/+}$ C5N keratinocytes. (C-D) Single or combined treatment of BSZ2 (C) or ASZ001 cells (D) with cyclopamine and gefitinib, GANT61 and gefitinib, or cyclopamine and JUN shRNA (siJUN), respectively; cyc: cyclopamine, gef: gefitinib. Statistical significance was determined by Student´s t-test. * $p < 0.05$, ** $p < 0.02$;